

Effective field theory approach to the gravitational two-body dynamics at fourth post-Newtonian order and quintic in the Newton constant

Stefano Foffa,^{1,*} Pierpaolo Mastrolia,^{2,†} Riccardo Sturani,^{3,‡} and Christian Sturm^{4,§}

¹*Département de Physique Théorique and Centre for Astroparticle Physics, Université de Genève, CH-1211 Geneva, Switzerland*

²*Dipartimento di Fisica ed Astronomia, Università di Padova, Via Marzolo 8, 35131 Padova, Italy and INFN, Sezione di Padova, Via Marzolo 8, 35131 Padova, Italy*

³*International Institute of Physics (IIP), Universidade Federal do Rio Grande do Norte (UFRN) CP 1613, 59078-970 Natal-RN, Brazil*

⁴*Universität Würzburg, Institut für Theoretische Physik und Astrophysik, Emil-Hilb-Weg 22, D-97074 Würzburg, Germany*

(Received 10 January 2017; published 8 May 2017)

Working within the post-Newtonian (PN) approximation to general relativity, we use the effective field theory (EFT) framework to study the conservative dynamics of the two-body motion at fourth PN order, at fifth order in the Newton constant. This is one of the missing pieces preventing the computation of the full Lagrangian at fourth PN order using EFT methods. We exploit the analogy between diagrams in the EFT gravitational theory and two-point functions in massless gauge theory, to address the calculation of four-loop amplitudes by means of standard multiloop diagrammatic techniques. For those terms which can be directly compared, our result confirms the findings of previous studies, performed using different methods.

DOI: [10.1103/PhysRevD.95.104009](https://doi.org/10.1103/PhysRevD.95.104009)

I. INTRODUCTION

The post-Newtonian (PN) approximation to the two-body problem in general relativity has been the subject of intense investigation in the last decades as it describes the dynamics of gravitationally bound binary systems in the weak-curvature, slow-velocity regime, reviewed in Refs. [1–3].

From the phenomenological point of view its results have been of paramount importance in constructing the waveforms which were eventually used as templates [4,5] for the LIGO/Virgo data analysis pipeline leading to the detection of gravitational waves [6], along with numerical simulations to solve for the spacetime in the strong-curvature regime [7] and earlier in the analysis of the Hulse-Taylor pulsar arrival times [8,9].

Interferometric detectors of gravitational waves are particularly sensitive to the time-varying phase of the signal of coalescing binaries, which thus must be computed with better than $\mathcal{O}(1)$ precision [10]. Such a phase can be determined from short-circuiting the information of the energy and luminosity function of binary inspirals with at least 3PN-order accuracy.

Focusing on the conservative sector of the two-body problem without spins (see Ref. [3] for results involving spins), we recall that within the effective field theory (EFT) formalism, initially proposed in Ref. [11] and reviewed in Refs. [3,12–14], the 1PN, 2PN [15] and 3PN [16] dynamics

have been computed, reproducing results obtained with more traditional methods; moreover the 4PN Lagrangian, quadratic in the Newton constant G_N , was first derived in the EFT framework [17].

The complete 4PN dynamics has been obtained recently by two groups within the Arnowitt-Deser-Misner Hamiltonian formalism [18,19] and by iterating the PN equation in the harmonic gauge in Refs. [20,21]; in both approaches an arbitrary coefficient was fixed by using results for the gravitational wave tail effect from self-force computations [22–24]. It is worth mentioning that the two results did not initially agree at orders G_N^4 and G_N^5 and, as it was argued in Ref. [25], the discrepancy has been overcome by a suitable regularization of the infrared and ultraviolet divergences in the approach based on the equations of motion, although the new regularization could not yet fix the value of the second ambiguity parameter in Ref. [21].

This work goes in the direction of providing a third-party computation with an independent methodology by filling in one of the missing pieces to obtain the full 4PN result within EFT methods. Using the virial relation $v^2 \sim G_N M/r$, where r and v are respectively the relative distance and velocity of the binary constituents and M is the total mass, the terms contributing to the 4PN-order dynamics can be parametrized as $G_N^{5-n} v^{2n}$ with $0 \leq n \leq 5$, with the leading term being the Newtonian potential, scaling simply as G_N . By following the path paved in Ref. [17], we present in this work some results concerning the G_N^5 order.

The Lagrangian contains in general terms with high derivatives of the dynamical variables: it is however

* stefano.foffa@unige.ch

† pierpaolo.mastrolia@pd.infn.it

‡ riccardo@iip.ufrn.br

§ Christian.Sturm@physik.uni-wuerzburg.de

possible to keep the equations of motion of second order without altering the dynamics by adding to the Lagrangian terms *quadratic* at least in the equations of motions tuned to cancel the high-derivative terms at the price of introducing additional terms with higher G_N powers, according to the standard procedure first proposed in Ref. [26] and dubbed the *double zero* technique. The G_N^5 sector of the Lagrangian receives contributions from G_N , G_N^2 and G_N^3 Lagrangian terms which are at least quadratic in accelerations (computed in Ref. [17] up to G_N^2) via the *double zero* trick, as well as from *genuine* G_N^5 terms: in the present article, we focus on the genuine G_N^5 contribution, that is terms that do not contain *ab initio* any power of velocity v or acceleration \dot{v} , and leave the very last contribution, coming from $\mathcal{O}(G_N^3 \dot{v}^2)$ terms, to a forthcoming paper dedicated to the whole G_N^3 sector.

In this work, we evaluate the 50 diagrams contributing to the classical effective Lagrangian in the gravitational theory at order G_N^5 . They are nontrivial integrals over 3-momenta which can be computed by means of multiloop diagrammatic techniques. We exploit the analogy between diagrams in the EFT gravitational theory and diagrams corresponding to two-point functions in massless gauge theory, to address the calculation of the $\mathcal{O}(G_N^5)$ diagrams as two-point four-loop dimensionally regulated integrals in d dimensions. In particular, we use integration-by-parts identities (IBPs) [27–29] in two ways: according to the topology of the graph, IBPs allow to carry out the multiloop integration recursively loop by loop; alternatively, they can be used to express the result of the amplitudes as linear combinations of irreducible integrals, known as *master integrals* (MIs). The latter are evaluated independently. The contribution to the three-dimensional Lagrangian coming from each graph is then determined by taking the $d \rightarrow 3$ limit of the Fourier transform to position space.

The paper is organized as follows. In Sec. II we review the EFT formalism applied to the two-body dynamics in the PN approximation to general relativity and in Sec. III we present the details of the 4PN computation at G_N^5 order. We summarize in Sec. IV and conclude in Sec. V. Appendix A contains the expressions of the master integrals needed for the computation, in Appendix B we give the contribution to the Lagrangian coming from the individual diagrams and in Appendix C details of the computation of selected amplitudes are reported.

II. THE METHOD

The application of the EFT framework to post-Newtonian calculations in binary dynamics has now been extensively investigated. It was first formulated in this context in Ref. [11] and subsequently applied to various aspects of the binary problem (see Refs. [3,13] and references therein).

We summarize here the basic features of this approach, along the lines and notations of Refs. [16,17], while

referring the reader to the literature for a more complete account. The starting point is the action

$$S = S_{\text{bulk}} + S_{pp}, \quad (1)$$

with the worldline point-particle action representing the binary components (we only consider here spinless point masses and neglect tidal effects)

$$\begin{aligned} S_{pp} &= -\sum_{i=1,2} m_i \int d\tau_i \\ &= -\sum_{i=1,2} m_i \int \sqrt{-g_{\mu\nu}(x_i)} dx_i^\mu dx_i^\nu, \end{aligned} \quad (2)$$

as well as the usual Einstein-Hilbert action¹ plus a gauge-fixing term

$$S_{\text{bulk}} = 2\Lambda^2 \int d^{d+1}x \sqrt{-g} \left[R(g) - \frac{1}{2} \Gamma_\mu \Gamma^\mu \right], \quad (3)$$

which corresponds to the same harmonic gauge condition adopted in Refs. [1,20], where $\Gamma^\mu \equiv g^{\rho\sigma} \Gamma_{\rho\sigma}^\mu$. Here $\Lambda^{-2} \equiv 32\pi G_N L^{d-3}$, where G_N is the three-dimensional Newton constant and L is an arbitrary length scale which keeps the correct dimensions of Λ in dimensional regularization, and always cancels out in the expression of physical observables. In this framework, a Kaluza-Klein (KK) parametrization of the metric [30,31] is usually adopted (a somewhat similar parametrization was first applied within the framework of a PN calculation in Ref. [32]):

$$g_{\mu\nu} = e^{2\phi/\Lambda} \begin{pmatrix} -1 & A_j/\Lambda \\ A_i/\Lambda & e^{-c_d \phi/\Lambda} \gamma_{ij} - A_i A_j / \Lambda^2 \end{pmatrix}, \quad (4)$$

with, $\gamma_{ij} \equiv \delta_{ij} + \sigma_{ij}/\Lambda$, $c_d \equiv 2 \frac{(d-1)}{(d-2)}$ and i, j running over the d spatial dimensions. The field A_i is not actually needed in the present computation, so it will henceforth be set to zero; we refer the reader to Ref. [16] for the general treatment and formulas including A_i .

In terms of the metric parametrization (4), with $A_i = 0$, each worldline coupling to the gravitational degrees of freedom ϕ , σ_{ij} reads

$$\begin{aligned} S_{pp} &= -m \int d\tau \\ &= -m \int dt e^{\phi/\Lambda} \sqrt{1 - e^{-c_d \phi/\Lambda} \left(v^2 + \frac{\sigma_{ij}}{\Lambda} v^i v^j \right)}, \end{aligned} \quad (5)$$

and its Taylor expansion provides the various particle-gravity vertices of the EFT.

¹We adopt the ‘‘mostly plus’’ convention $\eta_{\mu\nu} \equiv \text{diag}(-, +, +, +)$, and the Riemann and Ricci tensors are defined as $R_{\nu\rho\sigma}^\mu = \partial_\rho \Gamma_{\nu\sigma}^\mu + \Gamma_{\alpha\rho}^\mu \Gamma_{\nu\sigma}^\alpha - \rho \leftrightarrow \sigma$, $R_{\mu\nu} \equiv R_{\mu\alpha\nu}^\alpha$.

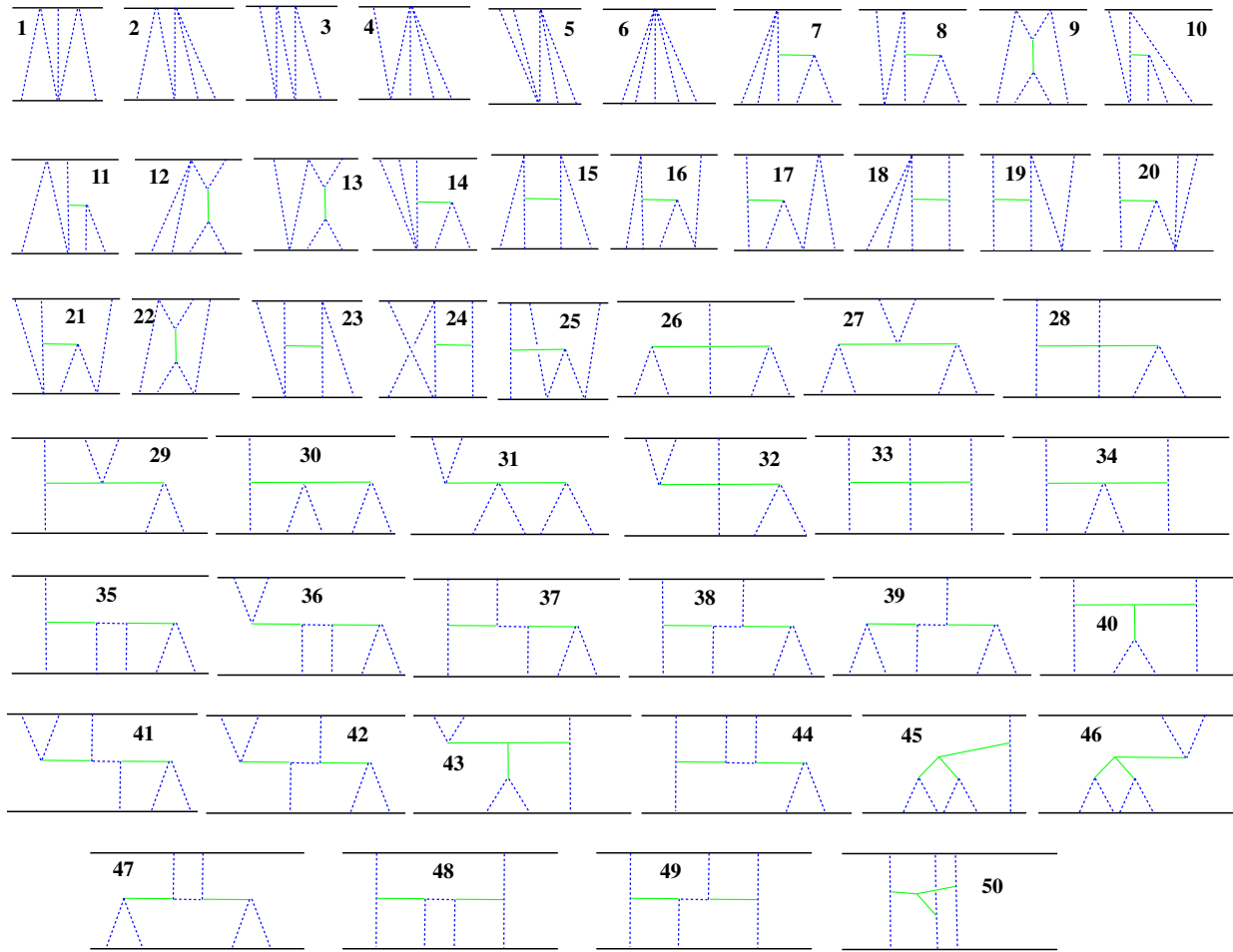


FIG. 1. The diagrams contributing at order G_N^5 . As in the EFT approach the massive objects are nondynamical: the horizontal black lines have to be seen as classical sources, and not as propagators. Green solid lines stand for σ field propagators, while blue dashed lines stand for ϕ fields.

Also the pure gravity sector $S_{\text{bulk}} = S_{EH} + S_{GF}$ can be explicitly written in terms of the KK variables; we report here only those terms which are needed for the present calculation²:

$$\begin{aligned}
 S_{\text{bulk}} \supset & \int d^{d+1}x \sqrt{\gamma} \left\{ \frac{1}{4} [(\vec{\nabla}\sigma)^2 - 2(\vec{\nabla}\sigma_{ij})^2] - c_d (\vec{\nabla}\phi)^2 \right. \\
 & - \frac{1}{\Lambda} \left(\frac{\sigma}{2} \delta^{ij} - \sigma^{ij} \right) (\sigma_{ik}{}^l \sigma_{jl}{}^k - \sigma_{ik}{}^k \sigma_{jl}{}^l \\
 & \left. + \sigma_{,i} \sigma_{jk}{}^k - \sigma_{ik,j} \sigma^k \right\}. \quad (6)
 \end{aligned}$$

The two-body effective action can be found by integrating out the gravity fields from the above-derived actions

²It is understood that spatial indices in this expression, including those implicit in terms carrying a $(\vec{\nabla})^2$, are contracted by means of the spatial metric γ_{ij} , which implies the appearance of extra σ fields, e.g. $(\vec{\nabla}\sigma)^2 \equiv \gamma^{ab} \gamma^{cd} \gamma^{ij} \sigma_{ab,i} \sigma_{cd,j}$ and $\gamma^{ij} = (\gamma^{-1})_{ij}$ (and in the second line $\sigma^{ij} = \sigma_{ij}$, $\sigma = \delta^{ij} \sigma_{ij}$).

$$\exp[iS_{\text{eff}}] = \int D\phi D\sigma_{ij} \exp[i(S_{\text{bulk}} + S_{pp})]. \quad (7)$$

As usual in field theory, the functional integration can be perturbatively expanded in terms of Feynman diagrams involving the gravitational degrees of freedom as internal lines only,³ regarded as dynamical fields emitted and absorbed by the point particles which are taken as nondynamical sources.

In order to make manifest the v scaling necessary to classify the results according to the PN hierarchy, it is convenient to work with the space-Fourier transformed fields

$$W_p^a(t) \equiv \int d^d x W^a(t, x) e^{-ip \cdot x} \quad \text{with } W^a = \{\phi, \sigma_{ij}\}. \quad (8)$$

³As we focus on the conservative part of the dynamics, we are not interested in diagrams where gravitational radiation is released to infinity, even though *tail* effects [33] involving emitted and absorbed radiation are relevant at G_N^2 order also in the conservative sector.

The fields defined above are the fundamental variables in terms of which we are going to construct the Feynman graphs; the action governing their dynamics can be found from Eqs. (5) and (6).

The next step is to lay down all the diagrams which contribute at this $\mathcal{O}(G_N^5)$ in the static limit, following the rule that each vertex involving n gravitational fields carries a factor $G_N^{n/2-1}$ if it is a bulk one, and a factor $G_N^{n/2}$ if it is attached to an external particle.

The diagrams in Fig. 1 schematically represent the exchange of gravitational potential modes through the field ϕ (blue dotted lines) and σ_{ij} (green solid line) which mediate the gravitational interaction. Massive objects represented by the thick horizontal black solid line are nondynamical sources or sinks of gravitational modes. Their dynamics is described by the worldline S_{pp} and hence no massive particle propagator is present in between two different insertions of gravitational modes on the same particle.

The amplitudes corresponding to each diagram can be built from the Feynman rules in momentum space derived from \mathcal{S}_{pp} , $\mathcal{S}_{\text{bulk}}$. By looking in particular at the quadratic parts, one can explicitly write the propagators:

$$P[W_p^a(t_a)W_{p'}^b(t_b)] = \frac{1}{2} P^{aa} \delta_{ab} (2\pi)^d \delta^d(p+p') \mathcal{P}(p^2, t_a, t_b) \delta(t_a - t_b), \quad (9)$$

where $P^{\phi\phi} = -\frac{1}{c_d}$, $P^{\sigma_{ij}\sigma_{kl}} = -(\delta_{ik}\delta_{jl} + \delta_{il}\delta_{jk} + (2-c_d)\delta_{ij}\delta_{kl})$ and

$$\mathcal{P}(p^2, t_a, t_b) = \frac{i}{p^2 - \partial_{t_a} \partial_{t_b}} \simeq \frac{i}{p^2} \quad (10)$$

has been truncated to its instantaneous nonrelativistic part. The terms involving time derivatives (which acting on the $e^{ip \cdot x}$, generate extra factors of v) can be indeed neglected. In fact, in the present work, we are interested in the pure 4PN G_N^5 contribution, which, by power counting, can be accessed in the limit of zero velocity and instantaneous interactions. In other words, gravitational-mode momenta have scalings of the types $(v/r, 1/r)$, and therefore the temporal component of their momenta can be neglected, since we are computing the $G_N^5 v^0$ sector.

From the previous discussion, one can derive the Feynman rules, respectively for the ϕ propagator,

$$\text{---} \overset{p}{\text{---}} \text{---} \rightarrow -\frac{i}{2c_d p^2} \quad (11)$$

and for the σ propagator,

$$\text{---} \overset{rj}{\text{---}} \overset{kl}{\text{---}} \text{---} \rightarrow \frac{i P^{\sigma_{rj}\sigma_{kl}}}{2p^2}. \quad (12)$$

The Feynman rules for the interaction vertices can be derived in a similar fashion and are reported below:

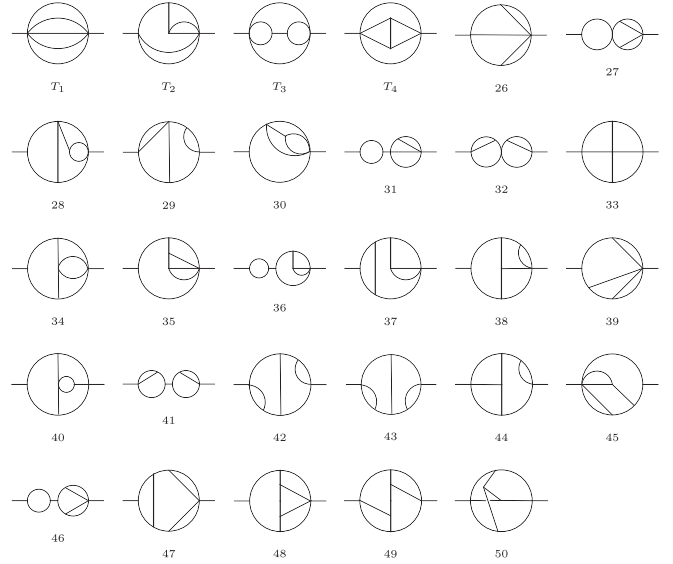


FIG. 2. Four-loop two-point topologies corresponding to the diagrams in Fig. 1.

$$\begin{aligned} & \text{---} \overset{p,rj}{\text{---}} \overset{p-k}{\text{---}} \overset{k}{\text{---}} \text{---} \\ & \rightarrow i \frac{2c_d}{\Lambda} \left[\frac{1}{2} (p-k) \cdot k \delta^{rj} - k^r (p-k)^j + (r \leftrightarrow j) \right], \\ & \text{---} \overset{p,q,rj}{\text{---}} \overset{k}{\text{---}} \overset{k+q,lm}{\text{---}} \text{---} \\ & \rightarrow i \frac{4c_d}{\Lambda^2} \left[k^r p^l \delta^{jlm} - \frac{1}{2} k^l p^m \delta^{rj} - \frac{1}{8} p \cdot k \mathcal{Q}^{rjlm} + (r \leftrightarrow j, l \leftrightarrow m) \right], \\ & \text{---} \overset{p,q,r}{\text{---}} \overset{p-k,q,r}{\text{---}} \overset{k,lm}{\text{---}} \text{---} \\ & \rightarrow i \frac{1}{8\Lambda} \left\{ (p-k) \cdot k \left(\frac{1}{2} \delta^{tr} \mathcal{I}^{lmjq} - \frac{1}{4} \delta^{qr} \mathcal{I}^{jlm} - \frac{1}{8} \delta^{tj} \mathcal{Q}^{qrilm} \right) + \right. \\ & \quad + \frac{1}{4} (p-k)^t k^j \mathcal{Q}^{qrilm} + \left[\left(\frac{1}{2} \delta^{tj} \delta^{mr} - \delta^{tr} \delta^{jm} \right) (p-k)^q k^l - (l \leftrightarrow q) \right] + \\ & \quad \left. + \delta^{lm} \delta^{tr} (p-k)^q k^j - \delta^{tm} \delta^{qr} (p-k)^l k^j + (t \leftrightarrow j, l \leftrightarrow m, q \leftrightarrow r) \right\}, \\ & \text{---} \overset{\dots}{\text{---}} \overset{\dots}{\text{---}} \text{---} \rightarrow -\frac{i}{n! \Lambda^n} \end{aligned} \quad (13)$$

with $\mathcal{I}^{ijlm} \equiv \delta^{il} \delta^{jm} + \delta^{im} \delta^{jl}$ and $\mathcal{Q}^{ijlm} \equiv \mathcal{I}^{ijlm} - \delta^{ij} \delta^{lm}$.

Finally, the contribution of each amplitude to the two-body Lagrangian \mathcal{L} can be derived from its Fourier transform,

$$\mathcal{L}_a = -i \lim_{d \rightarrow 3} \int \frac{d^d p}{(2\pi)^d} e^{ip \cdot r} \text{ [box diagram] }_a \quad (14)$$

where the box diagram stands for the generic diagram $a = 1, \dots, 50$ of Fig. 1, and p is the momentum transfer of the source.

III. AMPLITUDES AND FEYNMAN INTEGRALS

In general, within the EFT approach, since the sources (black lines) are static and do not propagate, any gravity amplitude of order G_N^ℓ can be mapped into a $(\ell - 1)$ -loop two-point function with massless internal lines and external momentum p , where $p^2 \equiv s \neq 0$,

$$\text{[box diagram]} = \text{[circle diagram]} \quad (15)$$

Accordingly, the 50 diagrams in Fig. 1 can be mapped onto the 29 topologies of Fig. 2, where the sets $T_1 = \{1, 2, 3, 4, 5, 6\}$, $T_2 = \{7, 8, 10, 11, 14, 16, 17, 20, 21, 25\}$, $T_3 = \{9, 12, 13, 22\}$, $T_4 = \{15, 18, 19, 23, 24\}$, collect the diagrams that share the same topology. For instance, the diagrams 1 to 6 of Fig. 1 correspond to integrals which have the same five denominators of the graph indicated by T_1 in Fig. 2, but different numerators, due to the different terms associated to 1,2,3 or 4 ϕ emission or absorption from the massive particle.

The representation of the gravity amplitudes as four-loop two-point integrals yields the possibility of evaluating the latter by means of by-now standard multiloop techniques based on IBPs [27,28].

Accordingly, we collect the 50 amplitudes of Fig. 1 in two sets, $\mathcal{A}_I = \{1:28, 31, 32, 35:37, 39, 41, 45:47\}$ and $\mathcal{A}_{II} = \{29, 30, 33, 34, 38, 40, 42, 43, 44, 48, 49, 50\}$, and address their computation separately.

The set \mathcal{A}_I contains diagrams with a simpler internal structure, and they have been computed by using the kite rule [27,28]

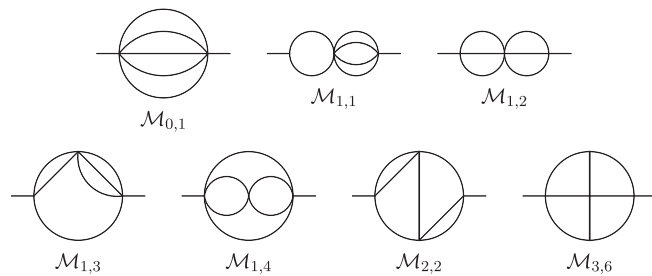


FIG. 3. The master integrals which appear in the calculation of the amplitudes in the set \mathcal{A}_{II} . The names of the diagrams follow Refs. [36–38].

$$\frac{(4-d)}{2} \text{ [kite diagram]} = \text{[circle with dot]} - \text{[two circles]} \quad (16)$$

where the dots stand for squared denominators, and by using the standard identity holding for two-point one-loop graphs,

$$\int \frac{d^d k}{(2\pi)^d} \frac{1}{k^{2a}(p-k)^{2b}} = \text{[circle with dots]} = \frac{(p^2)^{d/2-a-b}}{(4\pi)^{d/2}} \frac{\Gamma(d/2-a)\Gamma(d/2-b)\Gamma(a+b-d/2)}{\Gamma(a)\Gamma(b)\Gamma(d-a-b)} \quad (17)$$

where a and b are generic denominators' powers. Alternatively we also performed an IBP reduction using the program REDUZE [34,35], identifying five MIs, namely $\mathcal{M}_{0,1}$, $\mathcal{M}_{1,1}$, $\mathcal{M}_{1,2}$, $\mathcal{M}_{1,3}$, $\mathcal{M}_{1,4}$ of Fig. 3. Both strategies gave the same results.

The amplitudes \mathcal{A}_{II} , instead, have a less trivial internal structure. By means of IBPs, they have been systematically reduced to linear combinations of seven MIs, all shown in Fig. 3. In this case, the reduction to MIs has been performed in two ways: by an in-house implementation of Laporta's algorithm which is based on FORM [39–41], as well as by means of REDUZE.

The four-loop MIs in Fig. 3 can be considered as a complete set of independent integrals, such that any amplitude of the sets \mathcal{A}_I and \mathcal{A}_{II} can be written as a linear combination of them. The results of the four-loop MIs in $d = 4 + \varepsilon$ Euclidean spacetime dimensions have been well known for some time [36,37], while the values around $d = 3 + \varepsilon$ of $\mathcal{M}_{2,2}$, $\mathcal{M}_{3,6}$ became available more recently [38]. In particular, $\mathcal{M}_{0,1}$, $\mathcal{M}_{1,1}$, $\mathcal{M}_{1,2}$, $\mathcal{M}_{1,3}$, $\mathcal{M}_{1,4}$ can be computed in a straightforward way by means of Eq. (17), and admit closed analytic expressions, exact in d , which can be expanded in a Laurent series in ε around $d = 3$. The series expansions of $\mathcal{M}_{2,2}$ and $\mathcal{M}_{3,6}$ were first obtained numerically in Ref. [38] by using the *difference equations method*, exploiting the fact that dimensionally regulated Feynman integrals obey dimensional recurrence relations [29,42–45]. For instance, owing to IBPs, $\mathcal{M}_{3,6}$ is a solution of the following recursive formula:

$$\frac{1}{(4\pi)^4} \cdot \text{[M}_{3,6}\text{]} \Big|_{d=2} = a_1 \text{[M}_{1,3}\text{]} + a_2 \text{[M}_{1,1}\text{]} + a_3 \text{[M}_{1,2}\text{]} + a_4 \text{[M}_{1,4}\text{]} + a_5 \text{[M}_{0,1}\text{]} \quad (18)$$

$$c_1 = \frac{(d-3)^2(d-2)^2s^2}{(d-4)^2(5d-14)(12-5d)}, \quad (28)$$

$$c_2 = \frac{(d-2)^2(432-512d+203d^2-27d^3)s}{8(d-4)^3(5-2d)(5d-12)}, \quad (29)$$

$$c_3 = \frac{(d-2)^2(76-58d+11d^2)s}{4(d-4)^2(14-5d)(5d-12)}, \quad (30)$$

$$c_4 = \frac{(d-2)^2s}{2(d-4)^2}, \quad (31)$$

$$c_5 = \frac{(d-2)^2(1096-1598d+870d^2-210d^3+19d^4)}{(d-4)^4(3-d)(3d-8)}. \quad (32)$$

This result can be expanded around $d = 3 + \varepsilon$, using the expressions of the MIs given in Appendix A,

$$\begin{aligned} \mathcal{A}_{49} = & -i(8\pi G_N)^5 (m_1 m_2)^3 2^{-4} (4\pi)^{-(4+2\varepsilon)} e^{2\varepsilon\gamma_E} s^{(1+2\varepsilon)} \\ & \times \left[\frac{1}{\varepsilon} \left(\frac{\pi^2}{16} - \frac{2}{3} \right) + \frac{29}{18} - \frac{13}{144} \pi^2 - \frac{\pi^2}{8} \log 2 + \mathcal{O}(\varepsilon) \right], \end{aligned} \quad (33)$$

where $\gamma_E = 0.57721\dots$ is the Euler-Mascheroni constant. Finally, by means of the Fourier transform formula

$$\int_p e^{ip \cdot r} p^{-2a} = \frac{\Gamma(d/2 - a)}{(4\pi)^{d/2} \Gamma(a)} \left(\frac{r}{2} \right)^{(2a-d)}, \quad (34)$$

one obtains the following Lagrangian term:

$$\mathcal{L}_{49} = -i \lim_{d \rightarrow 3} \int_p e^{ip \cdot r} \mathcal{A}_{49} = (32 - 3\pi^2) \frac{G_N^5 m_1^3 m_2^3}{r^5}. \quad (35)$$

IV. RESULTS AND DISCUSSION

The complete 4PN, $\mathcal{O}(G_N^5)$ Lagrangian was already presented in Ref. [20],

$$\begin{aligned} \mathcal{L}_{4PN}^{G_N^5} = & \frac{3}{8} \frac{G_N^5 m_1^5 m_2}{r^5} + \frac{G_N^5 m_1^4 m_2^2}{r^5} \left[\frac{1690841}{25200} + \frac{105}{32} \pi^2 \right. \\ & \left. - \frac{242}{3} \log \frac{r}{r'_1} - 16 \log \frac{r}{r'_2} \right] \\ & + \frac{G_N^5 m_1^3 m_2^3}{r^5} \left[\frac{587963}{5600} - \frac{71}{32} \pi^2 - \frac{110}{3} \log \frac{r}{r'_1} \right] \\ & + (m_1 \leftrightarrow m_2), \end{aligned} \quad (36)$$

where r'_1, r'_2 are two UV scales which do not contribute to physical observables. Such a Lagrangian gets contributions from the 50 genuine $\mathcal{O}(G_N^5)$ diagrams depicted in Fig. 1, and from diagrams at lower orders in G_N which are at least quadratic in the accelerations:

$$\mathcal{L}_{4PN}^{G_N^5} = \sum_{a=1}^{50} \mathcal{L}_a + \sum_{j=1}^3 \mathcal{L}_{4PN}^{G_N^j \rightarrow G_N^5} + (m_1 \leftrightarrow m_2). \quad (37)$$

The evaluation of $\sum_{a=1}^{50} \mathcal{L}_a$ represents the main result of this work, and it amounts to

$$\sum_{a=1}^{50} \mathcal{L}_a = \frac{3}{8} \frac{G_N^5 m_1^5 m_2}{r^5} + \frac{31}{3} \frac{G_N^5 m_1^4 m_2^2}{r^5} + \frac{141}{8} \frac{G_N^5 m_1^3 m_2^3}{r^5}. \quad (38)$$

The individual contributions \mathcal{L}_a are presented in Appendix B. We observe that, although there appear contributions which are divergent in the $d \rightarrow 3$ limit, the sum of all contributions is finite, and hence L does not show up in physical observables.

To obtain the whole expression for the 4PN $\mathcal{O}(G_N^5)$ corrections, one would need to add contributions generated from lower G_N terms when using the equations of motion, in order to eliminate terms quadratic at least in the accelerations. All such contributions have been computed also in the EFT framework [17], except for $\mathcal{L}_{4PN}^{G_N^3 \rightarrow G_N^5}$. We can nevertheless perform partial checks between Eq. (38) and Eq. (36).

A. The $m_1^5 m_2$ term

It can be proven that this term does not receive any contribution from lower G_N terms,⁵ and the corresponding coefficient for the two-body Lagrangian of Eq. (38) agrees with the Lagrangian term reported in Eq. (36).

B. The π^2 term.

The contributions coming from the lower G_N orders come entirely from the still unpublished $\mathcal{L}_{4PN}^{G_N^3 \rightarrow G_N^5}$: for dimensional reasons terms at least quadratic in the accelerations can appear only in $G_N^{m \leq n-1}$ sectors at n th PN order, and all the terms up to $\mathcal{O}(G_N^2)$ do not contain π^2 . Although the computational details will be given elsewhere, such

⁵Contributions to this term from lower G_N orders would come from terms of the type $G_N^{5-n} m_1^{5-n} m_2 a_2^n$ with $2 \leq n \leq 4$. However, diagrams giving rise to such terms would have exactly one propagator attached to particle 2, and hence a_2^2 or higher powers of a_2 can be taken out by integration by parts instead of by using the double zero trick. It was checked explicitly in Ref. [17] that $G_N^{5-n} m_1^{5-n} m_2 a_2^n$ terms do not appear in the Lagrangian for $n=3, 4$.

contributions have been computed in the EFT framework and are found to be

$$\frac{105}{32}\pi^2\frac{G_N^5m_1^4m_2^2}{r^5}-\frac{71}{32}\pi^2\frac{G_N^5m_1^3m_2^3}{r^5}. \quad (39)$$

This result, alone, already accounts for the Lagrangian π^2 term of Eq. (36), presented in Ref. [20] and previously computed also in Ref. [19]. Although some of the \mathcal{L}_a 's listed in Appendix B (namely, $a = 33, 49, 50$) contain terms proportional to π^2 , these terms cancel in the sum of all the diagrams (as shown in Ref. [46]), thus providing agreement with the literature.

C. Other terms

The other terms are not directly comparable without full knowledge of the $\mathcal{L}_{4PN}^{G_N^3 \rightarrow G_N^5}$ contribution, and without taking into account the different regularization schemes used here and in Ref. [20].

V. CONCLUSION

Working within the PN approximation to general relativity, we studied the conservative dynamics of the two-body motion at 4PN order, at fifth order in the Newton constant G_N , within the EFT framework. We determined an essential contribution of the complete 4PN Lagrangian at $\mathcal{O}(G_N^5)$, coming from 50 Feynman diagrams. By exploiting the analogy between such diagrams in the EFT gravitational theory and two-point four-loop functions in massless gauge theory, we addressed their calculation by means of multiloop diagrammatic techniques, based on integration-by-parts identities and difference equations. We performed the calculation within the dimensional regularization scheme, and the contribution to the Lagrangian of each graph was given as a Laurent series in $d = 3 + \epsilon$, where d is the number of dimensions. Although some individual amplitudes are divergent in the $\epsilon \rightarrow 0$ limit and others contain the irrational factor π^2 , the sum of the 50 terms is found to be finite at $d = 3$ and rational, in agreement with previous calculations performed with other techniques.

ACKNOWLEDGMENTS

We thank Luc Blanchet, Thibault Damour, Guillaume Faye and Ulrich Schubert-Mielnik for clarifying discussions, and Andreas von Manteuffel for kind correspondence on the use of REDUZE. We wish to thank ICTP-SAIFR, supported by FAPESP Grant No. 2016/01343-7, for the organization of the workshop ‘‘Analytic methods in General Relativity’’, where many stimulating discussions took place. The work of R.S. has been supported for most of the duration of the present work by the FAPESP Grant No. 2012/14132-3 and by the High

Performance Computing Center at UFRN. S.F. is supported by the Fonds National Suisse and by the SwissMap NCCR.

Note added.—In a first version of this manuscript, \mathcal{L}_{50} appeared to have a different value, leading to a disagreement with the literature. Subsequently, the authors of Ref. [46] pointed us to a missing overall factor of ‘‘−3’’ in \mathcal{L}_{50} , which we have been able to find and correct: the value of \mathcal{L}_{50} reported in this version is the amended one. Let us also note, that the analytic result for the master integral $\mathcal{M}_{3,6}$ obtained in Ref. [46] agrees with the semi-analytic expression given in our current work.

APPENDIX A: MASTER INTEGRALS

In this appendix, we provide the expressions of the master integrals. They are defined by

$$\begin{aligned} \mathcal{M}_{0,1} &= \int_{k_{1\dots 4}} \frac{1}{D_{1\dots 4}D_{14}}, & \mathcal{M}_{1,1} &= \int_{k_{1\dots 4}} \frac{1}{D_{1\dots 4}D_9D_{12}}, \\ \mathcal{M}_{1,2} &= \int_{k_{1\dots 4}} \frac{1}{D_{1\dots 4}D_{10}D_{11}}, & \mathcal{M}_{1,3} &= \int_{k_{1\dots 4}} \frac{1}{D_{1\dots 4}D_8D_{10}}, \\ \mathcal{M}_{1,4} &= \int_{k_{1\dots 4}} \frac{1}{D_{1\dots 4}D_7D_{13}}, & \mathcal{M}_{2,2} &= \int_{k_{1\dots 4}} \frac{1}{D_{1\dots 4}D_{10}D_{15}D_{16}}, \\ \mathcal{M}_{3,6} &= \int_{k_{1\dots 4}} \frac{1}{D_{1\dots 4}D_5D_6D_{10}D_{14}}, \end{aligned}$$

where k_i ($i = 1, 2, 3, 4$) are the loop momenta and p is the external momentum of the diagrams depicted in Fig. 3. The integral measure is the same as that used in Sec. III and is given by $\int_{k_{1\dots 4}} = \int_{k_1} \int_{k_2} \int_{k_3} \int_{k_4}$ with $\int_{k_i} \equiv \int \frac{d^d k_i}{(2\pi)^d}$ ($i = 1, 2, 3, 4$). The denominators read

$$\begin{aligned} D_{1\dots 4} &= k_1^2 k_2^2 k_3^2 k_4^2, & D_5 &= (k_2 - k_3)^2, \\ D_6 &= (k_1 - k_4)^2, & D_7 &= (k_2 + k_3 - k_4)^2, \\ D_8 &= (k_1 + k_2 + k_3 - k_4)^2, & D_9 &= (k_1 - p)^2, \\ D_{10} &= (k_1 + k_2 - p)^2, & D_{11} &= (k_3 + k_4 + p)^2, \\ D_{12} &= (k_2 - k_3 - k_4 + p)^2, & D_{13} &= (k_1 - k_2 - k_3 + p)^2, \\ D_{14} &= (k_1 + k_2 - k_3 - k_4 - p)^2, & D_{15} &= (k_1 + k_4 - p)^2, \\ D_{16} &= (k_2 + k_3 - p)^2. \end{aligned}$$

1. Master integrals known in d dimensions

The following master integrals are known in closed analytical form, exact in d :

$$\mathcal{M}_{0,1} = (4\pi)^{-2d} s^{2d-5} \frac{\Gamma(5-2d)\Gamma(\frac{d}{2}-1)^5}{\Gamma(\frac{5}{2}d-5)} \quad (A1)$$

$$\begin{aligned}
\mathcal{L}_{44} &= -\frac{G_N^5 m_1^3 m_2^3}{r^5} \left[\frac{37}{75} + \frac{2}{5} \mathcal{P} \right], \\
\mathcal{L}_{48} &= \frac{G_N^5 m_1^4 m_2^2}{r^5} \left[\frac{578}{75} + \frac{8}{5} \mathcal{P} \right], \\
\mathcal{L}_{49} &= \frac{G_N^5 m_1^3 m_2^3}{r^5} (32 - 3\pi^2), \\
\mathcal{L}_{50} &= \frac{G_N^5 m_1^3 m_2^3}{r^5} \left(4\pi^2 - \frac{124}{3} \right), \tag{B1}
\end{aligned}$$

where the pole part $\mathcal{P} \equiv \frac{1}{\epsilon} - 5 \log \frac{r}{L_0}$ (with L_0 defined by $L = \sqrt{4\pi\epsilon^{\gamma_E}} L_0$) cancels exactly in the sum of all the terms.

Diagrams which are symmetric under (1 \leftrightarrow 2) exchange, i.e. 3, 5, 22, 23, 24, 32, 33, 41, 42, 43, 49, 50 have been multiplied by 1/2.

APPENDIX C: EVALUATION OF \mathcal{A}_{33} AND \mathcal{A}_{50}

We describe the evaluation of amplitudes 33 and 50 which, along with amplitude 49 already discussed in detail in Sec. III, are the only ones containing π^2 terms.

1. Amplitude 33

$$\begin{aligned}
\mathcal{A}_{33} &= \text{Diagram with two vertical lines and a horizontal line} \\
&= -i (8\pi G_N)^5 \left(\frac{(d-2)}{(d-1)} m_1 m_2 \right)^3 \text{Diagram with a circle and a cross} [N_{33}], \tag{C1}
\end{aligned}$$

with

$$\begin{aligned}
&\text{Diagram with a circle and a cross} [N_{33}] \\
&\equiv \int_{k_1, k_2, k_3, k_4} \frac{N_{33}}{k_1^2 k_2^2 k_3^2 k_4^2 k_{14}^2 p_{12}^2 p_{34}^2 p_{123}^2}, \tag{C2}
\end{aligned}$$

and

$$\begin{aligned}
N_{33} &\equiv k_3 \cdot k_4 (k_2 \cdot p_{12} k_1 \cdot p_{34} + k_1 \cdot k_2 p_{12} \cdot p_{34} \\
&\quad - k_1 \cdot p_{12} k_2 \cdot p_{34}) \\
&\quad + k_2 \cdot k_4 (k_1 \cdot p_{12} k_3 \cdot p_{34} + k_1 \cdot k_3 p_{12} \cdot p_{34} \\
&\quad - k_3 \cdot p_{12} k_1 \cdot p_{34}) \\
&\quad + k_1 \cdot k_4 (k_3 \cdot p_{12} k_2 \cdot p_{34} - k_2 \cdot p_{12} k_3 \cdot p_{34} \\
&\quad - k_2 \cdot k_3 p_{12} \cdot p_{34}) \\
&\quad + k_2 \cdot k_3 (k_4 \cdot p_{12} k_1 \cdot p_{34} + k_1 \cdot p_{12} k_4 \cdot p_{34}) \\
&\quad + k_1 \cdot k_3 (k_2 \cdot p_{12} k_4 \cdot p_{34} - k_4 \cdot p_{12} k_2 \cdot p_{34}) \\
&\quad + k_1 \cdot k_2 (k_4 \cdot p_{12} k_3 \cdot p_{34} - k_3 \cdot p_{12} k_4 \cdot p_{34}), \tag{C3}
\end{aligned}$$

where $p_{123} \equiv p - k_1 - k_2 - k_3$, $p_{ab} \equiv p - k_a - k_b$, $k_{14} \equiv k_1 - k_4$. By means of IBPs, we express the two-point amplitude in terms of MIs,

$$\begin{aligned}
\text{Diagram with a circle and a cross} [N_{33}] &= c_1 \text{Diagram with a circle and a cross} + c_2 \text{Diagram with two circles} + c_3 \text{Diagram with two circles} + \\
&\quad + c_4 \text{Diagram with a circle and a cross} + c_5 \text{Diagram with a circle and a cross} \tag{C4}
\end{aligned}$$

and

$$c_1 = \frac{(d-2)(3d-10)(d^2-12d+24)s^3}{4(d-3)(5d-16)(5d-14)(5d-12)}, \tag{C5}$$

$$\begin{aligned}
c_2 &= \frac{(d-2)}{4(d-4)^2(2d-5)(3d-10)(5d-12)} \\
&\quad \times (19d^4 + 225d^3 - 2708d^2 + 8140d - 7680)s, \tag{C6}
\end{aligned}$$

$$\begin{aligned}
c_3 &= \frac{(d-2)}{4(d-4)^2(d-3)(5d-16)(5d-14)(5d-12)} \\
&\quad \times (33d^5 - 44d^4 - 1936d^3 \\
&\quad + 11024d^2 - 22512d + 16128)s, \tag{C7}
\end{aligned}$$

$$c_4 = -\frac{2(d-2)(d^3+7d^2-55d+78)s}{(d-4)^2(d-3)(5d-12)}, \tag{C8}$$

$$\begin{aligned}
c_5 &= \frac{(d-2)(2d-5)}{2(d-4)^2(d-3)^2(3d-10)(3d-8)} \\
&\quad \times (3d^4 + 204d^3 - 1856d^2 + 5296d - 4944). \tag{C9}
\end{aligned}$$

This result can be expanded around $d = 3 + \epsilon$, using the expressions of the MIs given in Appendix A,

$$\begin{aligned} \mathcal{A}_{33} = & -i(8\pi G_N)^5 (m_1 m_2)^3 2^{-4} (4\pi)^{-(4+2\epsilon)} e^{2\epsilon\gamma_E} s^{(1+2\epsilon)} \\ & \times \left[\frac{1}{\epsilon} \left(\frac{\pi^2}{48} - \frac{1}{3} \right) + \frac{49}{18} - \frac{5\pi^2}{16} + \frac{7\pi^2}{8} \log 2 - \frac{37\zeta_3}{8} \right. \\ & \left. + \mathcal{O}(\epsilon) \right]. \end{aligned} \quad (\text{C10})$$

Finally, by applying the Fourier transform formula (34) to $-i\mathcal{A}_{33}$, one gets the result for \mathcal{L}_{33} reported in Appendix B.

2. Amplitude 50

Coming to amplitude 50, we have

$$\begin{aligned} \mathcal{A}_{50} = & \text{Diagram} \\ = & -i(8\pi G_N)^5 \left(\frac{(d-2)}{(d-1)} m_1 m_2 \right)^3 \text{Diagram} [N_{50}], \end{aligned} \quad (\text{C11})$$

with

$$\text{Diagram} [N_{50}] \equiv \int_{k_1, k_2, k_3, k_4} \frac{N_{50}}{k_1^2 k_2^2 k_3^2 k_4^2 k_{12}^2 k_{34}^2 \hat{k}_{24}^2 p_{13}^2 \hat{p}_{14}^2}, \quad (\text{C12})$$

and

$$\begin{aligned} N_{50} \equiv & (k_3 \cdot p_{13} k_{12} \cdot \hat{p}_{14} - k_{12} \cdot p_{13} k_3 \cdot \hat{p}_{14} \\ & - k_3 \cdot k_{12} p_{13} \cdot \hat{p}_{14}) \\ & \times (k_2 \cdot k_{34} k_1 \cdot k_4 + k_1 \cdot k_{34} k_2 \cdot k_4 - k_4 \cdot k_{34} k_1 \cdot k_2) \\ & + (k_{12} \cdot k_{34} p_{13} \cdot \hat{p}_{14} - k_{34} \cdot p_{13} k_{12} \cdot \hat{p}_{14} \\ & - k_{12} \cdot p_{13} k_{34} \cdot \hat{p}_{14}) \\ & \times (k_1 \cdot k_2 k_3 \cdot k_4 - k_1 \cdot k_3 k_2 \cdot k_4 - k_1 \cdot k_4 k_2 \cdot k_3) \\ & + (k_{34} \cdot p_{13} k_1 \cdot \hat{p}_{14} + k_1 \cdot p_{13} k_{34} \cdot \hat{p}_{14} \\ & - k_1 \cdot k_{34} p_{13} \cdot \hat{p}_{14}) \\ & \times (k_4 \cdot k_{12} k_2 \cdot k_3 - k_2 \cdot k_{12} k_3 \cdot k_4) \\ & + (k_1 \cdot k_{34} k_3 \cdot k_{12} + k_1 \cdot k_3 k_{12} \cdot k_{34} \\ & - k_1 \cdot k_{12} k_3 \cdot k_{34}) \\ & \times (k_2 \cdot \hat{p}_{14} k_4 \cdot p_{13} + k_2 \cdot p_{13} k_4 \cdot \hat{p}_{14}) \\ & + (k_2 \cdot k_{12} k_4 \cdot k_{34} - k_4 \cdot k_{12} k_2 \cdot k_{34}) \\ & \times (k_1 \cdot k_3 p_{13} \cdot \hat{p}_{14} - k_1 \cdot p_{13} k_3 \cdot \hat{p}_{14}) \\ & - 2k_1 \cdot k_4 k_3 \cdot k_{34} k_2 \cdot p_{13} k_{12} \cdot \hat{p}_{14} \\ & - 2k_1 \cdot p_{13} k_3 \cdot k_{34} (k_2 \cdot k_4 k_{12} \cdot \hat{p}_{14} + k_4 \cdot k_{12} k_2 \cdot \hat{p}_{14}) \\ & + k_1 \cdot \hat{p}_{14} k_4 \cdot k_{12} (k_2 \cdot k_{34} k_3 \cdot p_{13} - 2k_2 \cdot p_{13} k_3 \cdot k_{34}) \end{aligned}$$

$$\begin{aligned} & + k_2 \cdot k_4 k_{12} \cdot k_{34} (k_3 \cdot p_{13} k_1 \cdot \hat{p}_{14} + k_1 \cdot p_{13} k_3 \cdot \hat{p}_{14}) \\ & + 2k_1 \cdot k_4 k_{12} \cdot p_{13} (k_2 \cdot k_{34} k_3 \cdot \hat{p}_{14} - k_3 \cdot k_{34} k_2 \cdot \hat{p}_{14}) \\ & + 2k_1 \cdot k_{12} k_4 \cdot k_{34} (k_3 \cdot p_{13} k_2 \cdot \hat{p}_{14} + k_2 \cdot p_{13} k_3 \cdot \hat{p}_{14}) \\ & + 2k_3 \cdot \hat{p}_{14} k_{12} \cdot p_{13} (k_1 \cdot k_{34} k_2 \cdot k_4 - k_4 \cdot k_{34} k_1 \cdot k_2) \\ & + k_1 \cdot \hat{p}_{14} k_2 \cdot k_4 (k_3 \cdot k_{12} k_{34} \cdot p_{13} - 2k_3 \cdot k_{34} k_{12} \cdot p_{13}) \\ & + 2k_1 \cdot k_{12} k_3 \cdot k_4 (k_{34} \cdot p_{13} k_2 \cdot \hat{p}_{14} + k_2 \cdot p_{13} k_{34} \cdot \hat{p}_{14}) \\ & + k_2 \cdot k_4 (k_{34} \cdot \hat{p}_{14} k_3 \cdot k_{12} k_1 \cdot p_{13} \\ & + p_{13} \cdot \hat{p}_{14} k_1 \cdot k_{12} k_3 \cdot k_{34}) \\ & - k_1 \cdot \hat{p}_{14} k_2 \cdot k_{12} k_4 \cdot k_{34} k_3 \cdot p_{13}, \end{aligned} \quad (\text{C13})$$

where $k_{ab} \equiv k_a - k_b$, $\hat{k}_{24} \equiv k_2 + k_4$, $p_{13} \equiv p - k_1 - k_3$ and $\hat{p}_{14} \equiv p - k_1 + k_2 - k_3 + k_4$. By means of IBPs, we express the two-point amplitude in terms of MIs,

$$\begin{aligned} \text{Diagram} [N_{50}] = & c_1 \text{Diagram} + c_2 \text{Diagram} + c_3 \text{Diagram} + \\ & + c_4 \text{Diagram} + c_5 \text{Diagram} \end{aligned} \quad (\text{C14})$$

and

$$\begin{aligned} c_1 = & -\frac{(d-2)}{4(d-3)(2d-7)(5d-16)(5d-14)(5d-12)} \\ & \times (3d-10)(3d^3 - 41d^2 + 165d - 204)s^3, \end{aligned} \quad (\text{C15})$$

$$\begin{aligned} c_2 = & \frac{(d-2)}{2(d-4)^2(2d-5)(3d-10)(5d-12)} \\ & \times (51d^4 - 769d^3 + 4018d^2 - 8868d + 7080)s, \end{aligned} \quad (\text{C16})$$

$$\begin{aligned} c_3 = & \frac{(d-2)}{12(d-4)^2(d-3)(5d-16)(5d-14)(5d-12)} \\ & \times (164d^5 - 3543d^4 + 26298d^3 - 90056d^2 \\ & + 146592d - 92160)s, \end{aligned} \quad (\text{C17})$$

$$c_4 = -\frac{(d-2)(9d-23)(d^2-12d+24)s}{2(d-4)^2(d-3)(5d-12)}, \quad (\text{C18})$$

$$\begin{aligned} c_5 = & -\frac{(d-2)}{2(d-4)^3(d-3)^2(3d-10)(3d-8)} \\ & \times (609d^5 - 8946d^4 + 52176d^3 \\ & - 151096d^2 + 217360d - 124320). \end{aligned} \quad (\text{C19})$$

This result can be expanded around $d = 3 + \epsilon$, using the expressions of the MIs given in Appendix A,

$$\begin{aligned}
\mathcal{A}_{50} = & -i(8\pi G_N)^5 (m_1 m_2)^3 2^{-4} (4\pi)^{-(4+2\epsilon)} e^{2\epsilon \gamma_E} S^{(1+2\epsilon)} \\
& \times \left[\frac{1}{\epsilon} \left(\frac{31}{36} - \frac{\pi^2}{12} \right) - \frac{985}{216} + \frac{61\pi^2}{144} - \frac{3\pi^2}{4} \log 2 + \frac{37\zeta_3}{8} \right. \\
& \left. + \mathcal{O}(\epsilon) \right]. \tag{C20}
\end{aligned}$$

Finally, by applying the Fourier transform formula (34) to $-i\mathcal{A}_{50}$, one gets the result for \mathcal{L}_{50} reported in Appendix B.

-
- [1] L. Blanchet, *Living Rev. Relativ.* **5**, 3 (2002).
[2] T. Futamase and Y. Itoh, *Living Rev. Relativ.* **10**, 2 (2007).
[3] R. A. Porto, *Phys. Rep.* **633**, 1 (2016).
[4] A. Taracchini, Y. Pan, A. Buonanno, E. Barausse, M. Boyle, T. Chu, G. Lovelace, H. P. Pfeiffer, and M. A. Scheel, *Phys. Rev. D* **86**, 024011 (2012).
[5] P. Schmidt, F. Ohme, and M. Hannam, *Phys. Rev. D* **91**, 024043 (2015).
[6] B. P. Abbott *et al.* (Virgo and LIGO Scientific Collaborations), *Phys. Rev. Lett.* **116**, 061102 (2016).
[7] A. H. Mroué *et al.*, *Phys. Rev. Lett.* **111**, 241104 (2013).
[8] J. H. Taylor and J. M. Weisberg, *Astrophys. J.* **253**, 908 (1982).
[9] T. Damour, *Phys. Rev. Lett.* **51**, 1019 (1983).
[10] C. Cutler *et al.*, *Phys. Rev. Lett.* **70**, 2984 (1993).
[11] W. D. Goldberger and I. Z. Rothstein, *Phys. Rev. D* **73**, 104029 (2006).
[12] W. D. Goldberger, in *Les Houches Summer School - Session 86: Particle Physics and Cosmology: The Fabric of Space-time, Les Houches, France, 2006*, edited by F. Bernardeau, C. Grojean, and J. Dalibard (Elsevier, New York, 2007).
[13] S. Foffa and R. Sturani, *Classical Quantum Gravity* **31**, 043001 (2014).
[14] I. Z. Rothstein, *Gen. Relativ. Gravit.* **46**, 1726 (2014).
[15] J. B. Gilmore and A. Ross, *Phys. Rev. D* **78**, 124021 (2008).
[16] S. Foffa and R. Sturani, *Phys. Rev. D* **84**, 044031 (2011).
[17] S. Foffa and R. Sturani, *Phys. Rev. D* **87**, 064011 (2013).
[18] T. Damour, P. Jaranowski, and G. Schäfer, *Phys. Rev. D* **89**, 064058 (2014).
[19] T. Damour, P. Jaranowski, and G. Schäfer, *Phys. Rev. D* **91**, 084024 (2015).
[20] L. Bernard, L. Blanchet, A. Bohé, G. Faye, and S. Marsat, *Phys. Rev. D* **93**, 084037 (2016).
[21] L. Bernard, L. Blanchet, A. Bohé, G. Faye, and S. Marsat, *Phys. Rev. D* **95**, 044026 (2017).
[22] L. Blanchet, S. L. Detweiler, A. Le Tiec, and B. F. Whiting, *Phys. Rev. D* **81**, 084033 (2010).
[23] A. Le Tiec, L. Blanchet, and B. F. Whiting, *Phys. Rev. D* **85**, 064039 (2012).
[24] D. Bini and T. Damour, *Phys. Rev. D* **87**, 121501 (2013).
[25] T. Damour, P. Jaranowski, and G. Schäfer, *Phys. Rev. D* **93**, 084014 (2016).
[26] T. Damour and G. Schäfer, *Gen. Relativ. Gravit.* **17**, 879 (1985).
[27] F. V. Tkachov, *Phys. Lett. B* **100**, 65 (1981).
[28] K. G. Chetyrkin and F. V. Tkachov, *Nucl. Phys.* **B192**, 159 (1981).
[29] S. Laporta, *Int. J. Mod. Phys. A* **15**, 5087 (2000).
[30] B. Kol and M. Smolkin, *Classical Quantum Gravity* **25**, 145011 (2008).
[31] B. Kol and M. Smolkin, *Phys. Rev. D* **77**, 064033 (2008).
[32] L. Blanchet and T. Damour, *Ann. Inst. H. Poincaré Phys. Theor.* **50**, 377 (1989).
[33] L. Blanchet and T. Damour, *Phys. Rev. D* **37**, 1410 (1988).
[34] C. Studerus, *Comput. Phys. Commun.* **181**, 1293 (2010).
[35] A. von Manteuffel and C. Studerus, arXiv:1201.4330.
[36] P. A. Baikov and K. G. Chetyrkin, *Nucl. Phys.* **B837**, 186 (2010).
[37] R. N. Lee, A. V. Smirnov, and V. A. Smirnov, *Nucl. Phys.* **B856**, 95 (2012).
[38] R. N. Lee and K. T. Mingulov, *Comput. Phys. Commun.* **203**, 255 (2016).
[39] J. A. M. Vermaseren, arXiv:math-ph/0010025.
[40] J. A. M. Vermaseren, *Nucl. Phys. B, Proc. Suppl.* **116**, 343 (2003).
[41] M. Tentyukov and J. A. M. Vermaseren, *Comput. Phys. Commun.* **176**, 385 (2007).
[42] L. M. Milne-Thomson, *The Calculus of Finite Differences* (American Mathematical Society, Providence, 1981).
[43] S. E. Derkachov, J. Honkonen, and Y. M. Pis'mak, *J. Phys. A* **23**, 5563 (1990).
[44] O. V. Tarasov, *Phys. Rev. D* **54**, 6479 (1996).
[45] R. N. Lee, *Nucl. Phys.* **B830**, 474 (2010).
[46] T. Damour and P. Jaranowski, arXiv:1701.02645.
[47] H. R. P. Ferguson, D. H. Bailey, and S. Arno, *Math. Comput.* **68**, 351 (1999).
[48] K. S. Thorne, *Rev. Mod. Phys.* **52**, 299 (1980).